Glucagon-Like Peptide-1 Receptor Imaging for Localization of Insulinomas

Emanuel Christ,* Damian Wild,* Flavio Forrer, Michael Brändle, Rahel Sahli, Thomas Clerici, Beat Gloor, Ferdinand Martius, Helmut Maecke, and Jean Claude Reubi

Divisions of Endocrinology, Diabetology, and Clinical Nutrition (E.C., R.S.) and Visceral Surgery (B.G.), Inselspital, University Hospital of Bern, and Division of Cell Biology and Experimental Cancer Research (J.C.R.), Institute of Pathology, University of Bern, CH-3010 Bern, Switzerland; Division of Nuclear Medicine (D.W., F.F.), University Hospital of Basel, CH-4031 Basel, Switzerland; Institute of Nuclear Medicine (D.W.), University College Hospital, London W1T 3AA, United Kingdom; Divisions of Endocrinology, Diabetes, and Osteology (M.B.) and Visceral Surgery (T.C.), Kantonsspital St. Gallen, CH-9007 St. Gallen, Switzerland; Division of Internal Medicine (F.M.), Bruderholzspital, University of Basel, CH-4056 Basel, Switzerland; and Division of Radiochemistry (H.M.), University Hospital of Basel, CH-4031 Basel, Switzerland

Context: The surgical removal of insulinomas is hampered by difficulties to localize it using conventional radiological procedures. Recently these tumors were shown to exhibit a very high density of glucagon-like peptide-1 receptors (GLP-1R) *in vitro* that may be used as specific targets for *in vivo* receptor radiolabeling.

Objective: The objective of the study was to test the 111In-labeled GLP-1R agonist 111In-DOTA-exendin-4 in localizing insulinomas using single photon emission computed tomography in combination with computed tomography images.

Design: This was a prospective open-label investigation.

Setting: The study was conducted at three tertiary referral centers in Switzerland.

Patients: Patients included six consecutive patients with proven clinical and biochemical endogenous hyperinsulinemic hypoglycemia.

Intervention: ^{111}In-DOTA-exendin-4 was administered iv at a dose of about 90 MBq (30 μg peptide) over 5 min. Whole-body planar images of the abdomen were performed at 20 min, 4 h, 23 h, 96 h, and up to 168 h after injection. After surgical removal of the insulinomas, GLP-1R expression was assessed in the tumor tissue *in vitro* by GLP-1R autoradiography.

Main Outcome Measure: The detection rate of insulinomas was measured.

Results: In all six cases, the GLP-1R scans successfully detected the insulinomas identified using conventional methods in four cases. By using a γ-probe intraoperatively, GLP-1R detection permitted a successful surgical removal of the tumors in all patients, diagnosed histopathologically as five pancreatic and one extrapancreatic insulinomas. *In vitro* GLP-1R autoradiography showed a high density of GLP-1R in all tested insulinomas.

Conclusion: *In vivo* GLP-1R imaging is an innovative, noninvasive diagnostic approach that successfully localizes small insulinomas pre- and intraoperatively and that may in the future affect the strategy of insulinoma localization. **(*J Clin Endocrinol Metab* 94: 4398–4405, 2009)**

ISSN Print 0021-972X ISSN Online 1945-7197
Printed in U.S.A.

doi: 10.1210/jc.2009-1082 Received May 20, 2009. Accepted August 12, 2009.
First Published Online October 9, 2009
* E.C. and D.W. contributed equally to this work.

For editorial see page 4125

Abbreviations: ASVS, Angiography and intraarterial calcium stimulation and venous sampling; CT, computed tomography; GLP-1, glucagon-like peptide-1; GLP-1R, GLP-1 receptor; MRI, magnetic resonance imaging; SPECT, single photon emission computed tomography; sst, somatostatin receptor.

The most common cause of endogenous hyperinsulinemic hypoglycemia in adults is an insulinoma (1). This neoplasm is typically small, benign in over 90% of the cases and usually located within the pancreas (1). The biochemical diagnosis of hyperinsulinemic hypoglycemia with neuroglycopenic symptoms is mandatory to proceed to imaging studies aimed at tumor localization (2, 3). Conventional imaging studies [*i.e.* magnetic resonance imaging (MRI), computed tomography (CT), endoscopic ultrasound] are the cornerstone of localization diagnosis of suspected insulinoma (4, 5). Due to the small size of the insulin-secreting tumors, these techniques have limited sensitivity (4–6). Methods such as angiography and intraarterial calcium stimulation and venous sampling (ASVS) have been shown to improve the sensitivity but are invasive procedures with concomitant risk for complications (6–8).

Recently new tumor imaging methods based on peptide receptor targeting have been successfully introduced (9). For instance, based on the marked overexpression of somatostatin receptors (sst) in neuroendocrine tumors, somatostatin receptor targeting has been introduced as *in vivo* diagnostic and therapeutic procedure in many of those neuroendocrine tumors (10, 11). Unfortunately, somatostatin receptors, in particular sst_2, are insufficiently expressed in many insulinomas (12), explaining the low rate of detection with somatostatin receptor scintigraphy (OctreoScan, Mallinckrodt, Petten, The Netherlands) (10). However, another peptide receptor, glucagon-like peptide-1 (GLP-1) receptor (GLP-1R), has recently been brought up in relation with insulinomas (12). GLP-1R is a peptide hormone receptor and a member of the glucagon receptor family (13, 14). GLP-1 or its analog, exenatide (Byetta, Lilly, Indianapolis, IN), is known to enhance insulin secretion in the β-cell and has been introduced in the therapy of type 2 diabetes (15, 16). Remarkably GLP-1R is expressed in very high density in almost all insulinomas (12) and may therefore be regarded as an interesting potential target.

Treatment strategy of insulinoma relies on surgical removal of the tumor if possible by a simple enucleation of the tumor. The precise preoperative but also the exact intraoperative localization of the insulinoma is critical to minimize the surgical intervention (5). GLP-1 like radioligands retaining high binding affinity to GLP-1R were recently developed including the specific ligand [Lys^{40}(Ahx-DOTA)NH_2]exendin-4 labeled with the radioisotope indium-111 (^{111}In-DOTA-exendin-4). Data in rodents (17) and preliminary data in humans (18) indicate that GLP-1 imaging using ^{111}In-DOTA-exendin-4 is capable to localize insulinoma *in vivo*. This report summarizes the clinical characteristics, imaging studies and invasive procedures of six consecutive patients with insulinoma in whom GLP-1R imaging has been performed.

Patients and Methods

Study patients and design

In this prospective pilot study, six consecutive patients (four females, two males) were recruited at three tertiary referral centers in Switzerland. Only patients with biochemically proven endogenous hyperinsulinemic hypoglycemia with neuroglycopenic symptoms, inadequately high serum insulin and C-peptide concentrations, and a negative screening for sulfonylurea were included in this trial (Table 1). In addition to the conventional preoperative localization methods, which were performed at the respective centers, all patients underwent GLP-1R scintigraphy maximally 14 d before elective surgery. Tumor tissue samples obtained during surgery were used for histopathological diagnosis and for GLP-1R and somatostatin receptor quantification.

The study was approved by the local ethical committee (Ethikkommission beider Basel), and written consent was obtained in accordance with provisions of the Declaration of Helsinki.

Synthesis and radiolabeling of DOTA-exendin-4

Lys^{40}(Ahx-DOTA)NH_2 exendin-4 (DOTA-exendin-4), a modification of exendin-4 (exenatide) was GMP custom synthesized by AnaSpec, Inc. (San Jose, CA). DOTA was thereby coupled via the Lys side chain of the C-terminally extended exendin-4 using Ahx as the spacer between DOTA and the peptide (19). The peptide conjugate was characterized by matrix assisted laser desorption ionization-mass spectrometry measurements that were done on a Voyager sSTR equipped with a Nd:YAG laser (355 nm) (Applied BioSystems, Framingham, MA).

An aliquot of 50 ml (50 μg) DOTA-exendin-4 was dissolved in 800 ml ammonium acetate buffer [0.2 M (pH 5.0)], incubated with 190 MBq high specific $^{111}InCl_3$ (Mallinckrodt, Petten, The Netherlands) at 95C for 5 min in the microwave oven (Biotage Initiator, Uppsala, Sweden) and then subjected to quality control by analytic HPLC (17).

GLP-1R imaging

Total-body planar images and single photon emission computed tomography (SPECT) in combination with CT scans of the abdomen were performed at 20 min, 4 h, and 23 h after iv injection of 30 μg (82–97 MBq) ^{111}In DOTA-exendin-4. Blood samples were taken at 1, 5, 15, 40, 60, 120, 180, and 240 min after injection to measure blood glucose levels and blood clearance of ^{111}In-DOTA-exendin-4.

In patients 2–6, one additional total-body and SPECT/CT scan was carried out at a late time point between 3 and 7 d after injection. Imaging was performed using a dedicated Symbia T2 hybrid SPECT/CT unit (Siemens Healthcare, Munich, Germany) equipped with a medium-energy, parallel-hole collimator (window setting 172 and 247 keV; width 15%; $2 \times 180°$ rotation; 64 projections; 128×128 matrix; 20 sec acquisition time per projection).

Low-dose CT imaging (130 kVp, 40 mAs) was carried out to correct for attenuation effects and to provide better anatomical localization of SPECT findings. Static total-body scans were used to calculate the effective half-life of ^{111}In-DOTA-exendin-4 in the tumor and kidneys.

Finally, all patients underwent γ probe guided surgery.

Conventional imaging and functional testing

MRI scans were performed in all patients using a three-phasic, breath-held T1 gadolinium-enhanced protocol. Four pa-

TABLE 1. Clinical characteristics and biochemical evaluation of six patients with insulinoma

	Patient 1	Patient 2	Patient 3	Patient 4	Patient 5	Patient 6
Clinical characteristics						
Age (yr)	31	64	49	55	44	72
Gender	F	M	F	F	F	M
Presenting symptom	Unconsciousness, A and E, hypoglycemia	Confusion, hypoglycemia during night, seizures?	Confusion at night with seizures	Confusion at night	Confusion in the morning, seizures?	Confusion, A and E, hypoglycemia
Duration of symptoms (months)	4	6	6	36	24	NA
Clinical and biochemical evaluation at the end of the fasting test						
Duration of fasting (h)	19	20	7	11	27	13
Leading symptom	Adrenergic symptoms, confusion	Confusion	Seizures, A and E	Confusion	Somnolence	Confusion
Glucose (mmol/liter)	1.6	2.1	1.9	1.3	1.5	1.9
C-peptide (nmol/liter)	1.4	1.7	0.8	0.8	0.8	1.0
Insulin (mU/liter)	5.9	38.6	11	5.1	14.8	13

F, female; M, male; A and E, Accident and Emergency Department; NA, not available.

tients (patients 1, 2, 5, 6) had additional dual-phase, thin-section multidetector CT scans. Endoscopic ultrasound was performed in all patients under mild analgesia as previously described (20). A selective ASVS was carried out in patients 2, 4, and 5 at the University Hospital of Zurich according to the local protocol that is described in details elsewhere (7). In patient 2, ^{111}In-pentetreotide total body scans were carried out 4 and 24 h after injection of 190 MBq ^{111}In-pentetreotide (OctreoScan).

Conventional imaging and GLP-1R scans were performed within 2 months.

Image reporting

All conventional scans were reported independently by experienced dedicated radiologists. Two nuclear medicine physicians visually assessed GLP-1R scans. Radiologists and nuclear medicine physicians were blinded to other imaging results but were aware of the patients' clinical history.

In vitro analysis of the insulinoma

GLP-1R expression was evaluated *in vitro* by GLP-1R autoradiography as previously reported using ^{125}I-GLP-1 (7–36)amide (74 Bq/mmol; Anawa, Wangen, Switzerland) as radioligand in sections of patients' tumor samples (21). The *in vitro* autoradiography of somatostatin receptor sst_1-sst_5 expression was performed in consecutive sections of the same tumor as previously described (22).

Role of the funding source

The sponsor of the study had no role in study design, data collection, data analysis, data interpretation, or writing of this manuscript. The corresponding author had full access to all the data in this study and had final responsibility for the decision to submit for publication.

Results

Clinical characteristics and biochemical investigations of the patients

The clinical characteristics and biochemical investigations are summarized in Table 1. Six patients volunteered for this study (four females, two males; age range 31–72 yr). All presented with neuroglycopenic symptoms ranging from confusion, unconsciousness, up to seizures. In three patients, neuroglycopenic symptoms lead to investigation in an accident and emergency department with documentation of hypoglycemia. The history of the patients revealed symptoms suggestive for hypoglycemia for 4–36 months prior to the diagnosis.

In all six patients, a fasting test was performed. Symptoms of neuroglycopenia in association with low plasma glucose levels (glucose range 1.3–2.1 mmol/liter) and increased insulin (5.1–38.6 mU/liter) and C-peptide (range 0.8–1.7 nmol/liter) levels occurred in all patients after 7–27 h of fasting.

Preoperative localization

The preoperative work-up is summarized in Table 2. CT imaging was performed in four patients showing a lesion only in one patient (patient 5). MRI was carried out in all six patients, revealing a lesion in one patient (patient 5). It has to be mentioned that in patient 2 (patient with an ectopic insulinoma), the tumor was diagnosed only retrospectively in the MRI after visualization of a suspicious lesion by GLP-1R imaging. Endoscopic ultrasound was performed in all patients

TABLE 2. Preoperative and intraoperative localization and therapy of the six patients with insulinoma

	Patient 1	Patient 2	Patient 3	Patient 4	Patient 5	Patient 6
Preoperative localization						
CT	−	−	NA	NA	+	−
MRI	−	−[a]	−	−	+	−
Endoscopic sonography	+	−	+	−	+	+
ASVS	NA	A. mes. sup.	NA	A. gastroduod.	A. pancr. dors.	NA
^{111}In-DOTA-exendin-4 SPECT/CT	+	+	+	+	+	+
Intraoperative localization						
Ultrasound	+	+[b]	+	+	+	+
γ -Probe-guided localization	+	+	+	+	+	+
Surgical procedure	Whipple	Enucleation ectopic lesion, Whipple	Enucleation	Enucleation	Enucleation	Enucleation
Tumor characteristics						
Histopathology	Insulinoma	Insulinoma	Insulinoma	Insulinoma	Insulinoma	Insulinoma
Dimension (mm)	12	13	17	11	18	9
Localization	Body tail transition	Ectopic, mesentery	Head of pancreas	Head of pancreas	Body tail transition	Tail
Receptor profile						
GLP-1R density (dpm/mg tissue; mean ± SEM, n ≥3)	5012 ± 495	2605 ± 340	>10,000	>10,000	4891 ± 498	NA[c]
sst expression	0	0	+[d]	0	+[d]	NA[c]

A. mes. sup., A. gastroduod., A. pancreatica dors., Significant rise in insulin levels after injection of calcium into the arteria mesenterica superior, arteria gastroduodenalis, arteria pancreatica dorsalis, respectively; sst, somatostatin receptor; NA, not available.

[a] Extrapancreatic lesion was retrospectively diagnosed after localization with ^{111}In-DOTA-exendin-4 SPECT/CT; [b] lesion discovered intraoperatively on the basis of knowledge of the findings of the ^{111}In-DOTA-exendin-4 SPECT/CT; [c] not enough tissue available for receptor determination; [d] subtype profile reveals low levels of sst_1 and sst_3.

showing a lesion in four of six patients. ASVS was performed in three patients, suggesting an insulinoma in the vascular territory of the anterior mesenteric artery (patient 2), gastroduodenal artery (patient 4), and the dorsal pancreatic artery (patient 5).

GLP-1R scintigraphy (Table 2 and Figs. 1–3)

The labeling yield of ^{111}In-DOTA-exendin-4 was greater than 98% at a specific activity of 20 GBq/μmol and a radiochemical purity of about 90%. The blood glucose levels after the ^{111}In-DOTA-exendin-4 injection are sum-

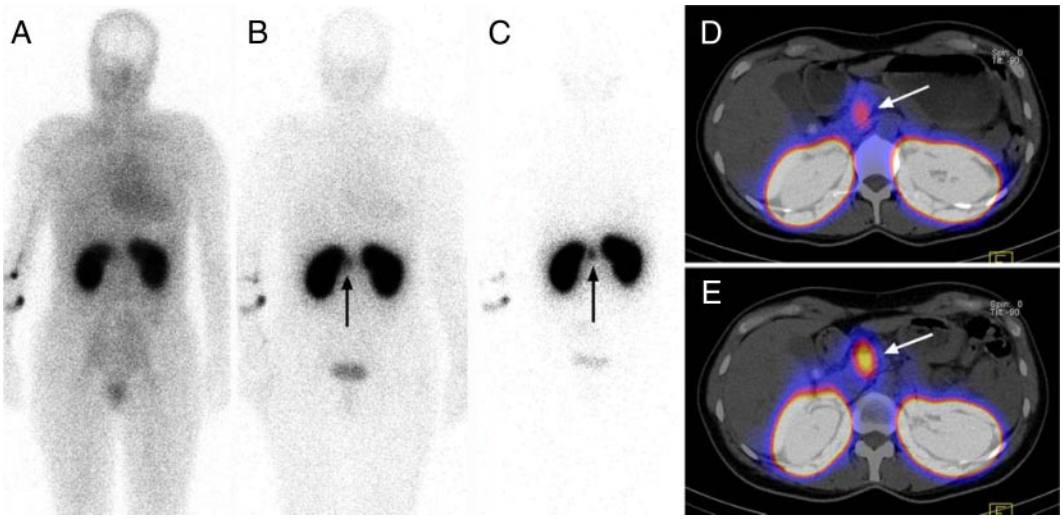

FIG. 1. ^{111}In-DOTA-exendin-4 whole-body planar images (A–C) and ^{111}In-DOTA-exendin-4 SPECT/CT images (D and E) from patient 3. Whole-body scans were carried out 20 min (A), 4 h (B), and 3 d (C) after injection, whereas SPECT/CT scans were performed 4 h (D) and 3 d (E) after injection of 97 MBq ^{111}In-DOTA-exendin-4. Four hours after injection, there is already focal ^{111}In-DOTA-exendin-4 uptake visible in the head of pancreas (*arrow*) on whole-body (B) and SPECT/CT (D) scans. The tumor to pancreas uptake ratio was 1.9 at 4 h after injection (D) and 3.2 at 3 d after injection of the radioligand. The longest residence times of ^{111}In-DOTA-exendin-4 were observed in the tumor (*arrow*) and kidneys (C).

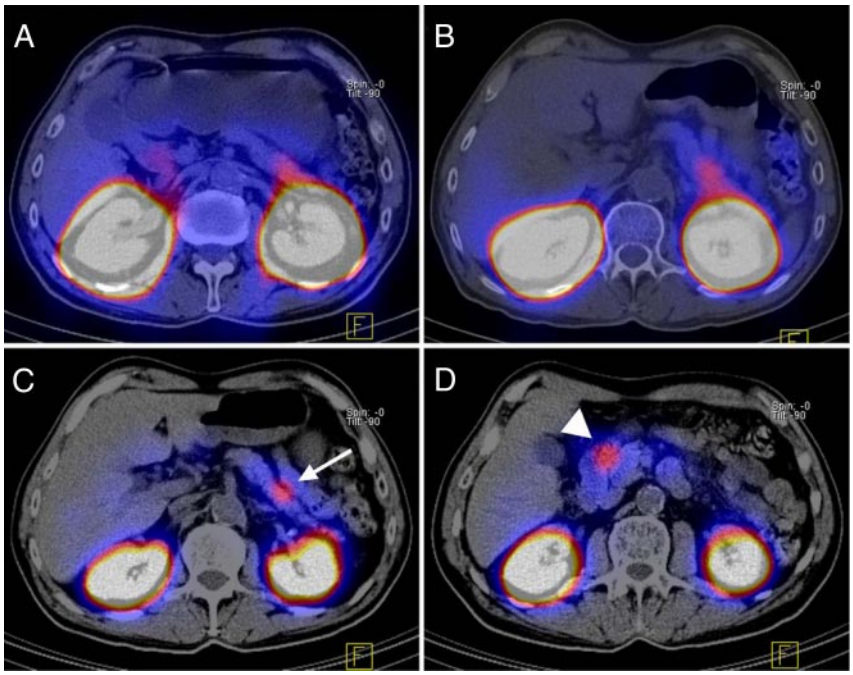

FIG. 2. ^{111}In-DOTA-exendin-4 SPECT/CT images from patient 6 at 4 h (A), 23 h (B), and 6 d (C and D) after injection of 88 MBq ^{111}In-DOTA-exendin-4. A demarcation between tumor in the tail of pancreas (*large arrow*) and left kidney was possible only at late scans 3 d after injection of the radioligand (A–C). The tumor to kidney uptake radio improved from 0.02 at 23 h (B) to 0.10 at 3 d after injection (C). Additional focal ^{111}In-DOTA-exendin-4 uptake was visible in the region of the proximal duodenum (*short arrow* in D). This finding may be related to the fact that the Brunner's gland of the duodenum expresses GLP-1R in high density. The corregistrated CT scan was important here for the localization and interpretation of this lesion.

marized in Table 3. The nadir of blood glucose levels occurred 40 min after the injection. The decrease in blood glucose levels was between 0.3 and 2.4 mmol/liter. An exogenous glucose infusion (5%) for maximum 120 min was necessary in three patients. The quantity of infused glucose varied from 10 g up to maximum 22.5 g. By regularly monitoring glucose levels after injection, no severe hypoglycemic episode occurred. One patient experienced a short episode of vomiting; otherwise, no further side effects were observed.

Blood sampling revealed a biexponential blood clearance of ^{111}In-DOTA-exendin-4: $t_{½} = 26 \pm 4$ min and $t_{½} = 85 \pm 5$ min; approximately 70% of the administered dose was cleared in the alpha phase. The clearance occurred exclusively via the kidneys. The longest residence times of ^{111}In-DOTA-exendin-4 were observed in the tumor and kidneys (Fig. 1C). The effective half-life of ^{111}In-DOTA-exendin-4 was longer in the tumor (38–64 h) than the kidneys (31.2–31.9 h).

Patients 1, 2, 3, and 5 showed intense ^{111}In-DOTA-exendin-4 uptake in the tumor just 4 h after injection (see for example patient 3 in Fig. 1, B and D). Patient 3 also demonstrated intense uptake at late scanning (see Fig. 1E), whereas patients 4 and 6 showed demarcation between tumor and kidney only at late scans 3–7 d after injection (*i.e.* see patient 6 in Fig. 2, A–C). Tumor to background ratio was high (>3) with the exception of the kidneys, which featured a high uptake. In patients 2 and 6, a small area of increased activity was observed in the region of the proximal duodenum (*i.e.* see patient 6 in Fig. 2D).

Importantly, GLP-1 scintigraphy correctly localized the insulinoma in all six patients (Table 2 and Figs. 1–3). In patients 1, 3, 5, and 6, the GLP-1R imaging was found to overlap with endoscopic ultrasound, and in patient 4, a GLP-1 scan confirmed the lesion localized by ASVS. In patient 2 the conventional imaging did not initially show a suspicious lesion. Although ASVS correctly suggested an insulinoma in the vascular territory of the anterior mesenteric artery in this patient, the ectopic origin of this insulinoma would not have been detected without GLP-1R imaging.

Intraoperative localization and surgical procedure

In all patients intraoperative palpation and ultrasound was performed that confirmed the findings of the preop-

TABLE 3. Blood glucose levels before and after injection of 30 μg (82–97 MBq) ^{111}In-DOTA-exendin-4

	Patient 1	Patient 2	Patient 3	Patient 4[a]	Patient 5[b]	Patient 6[a]
Baseline blood glucose level (mmol/liter)	4.2	6.1	4.7	3.8	3.6	4.1
Nadir of blood glucose level (mmol/liter)[c]	3.1	4.7	4.3	2.2		1.7
Blood glucose level 3 h after injection (mmol/liter)	7.3	6.0	5.5	5.2	5.2	4.9

[a] Patients 4 and 6 received 350 ml (patient 4) and 450 ml (patient 6) glucose (5%) by continuous iv injection 40–160 min after injection of the radiopeptide; [b] patient 5 received a total of 200 ml 5% glucose starting just before the injection of ^{111}In-DOTA-exendin-4, and because this patient did not show a decrease in blood glucose levels within 60 min, the infusion was stopped; [c] in patients 1, 2, 3, 4, and 6, the lowest blood glucose level was measured 40 min after injection of ^{111}In-DOTA-exendin-4.

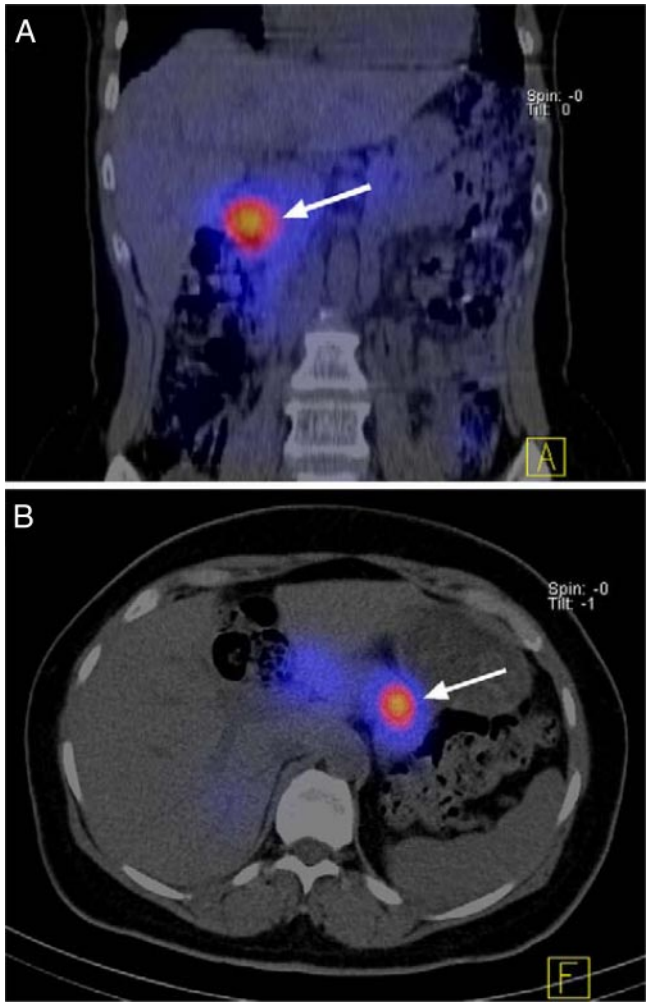

FIG. 3. Coronal SPECT/CT image from patient 4 (A) and transaxial SPECT/CT image from patient 5 (B) at 3 d after injection of about 90 MBq ^{111}In-DOTA-exendin-4. In patient 4 the insulinoma is located in the head of pancreas (*arrow*), whereas in patient 5 the insulinoma is visible in the body-tail transition of the pancreas (*arrow*). The tumor to pancreas uptake ratio was greater than 3 in both patients.

erative GLP-1R scans. In patient 2, however, it was extremely difficult to detect the lesion by ultrasound. Importantly, in all patients the tumor was correctly localized *in situ* with a γ-probe up to 14 d after injection of ^{111}In-DOTA-exendin-4. The intraoperative findings allowed proceeding to an enucleation of the tumor in four of six patients. In patient 1 a Whipple procedure was performed due to the anatomical site of the lesion. In patient 2 malignant insulinoma could not be excluded by the time of surgery, and the ASVS suggested a lesion within the head of pancreas. However, histological work-up of the whole surgical preparation of patient 2, including head of the pancreas and duodenum, did not reveal an additional neuroendocrine tumor, thereby confirming an ectopic origin of the insulinoma in the mesentery between duodenum and superior mesenteric artery.

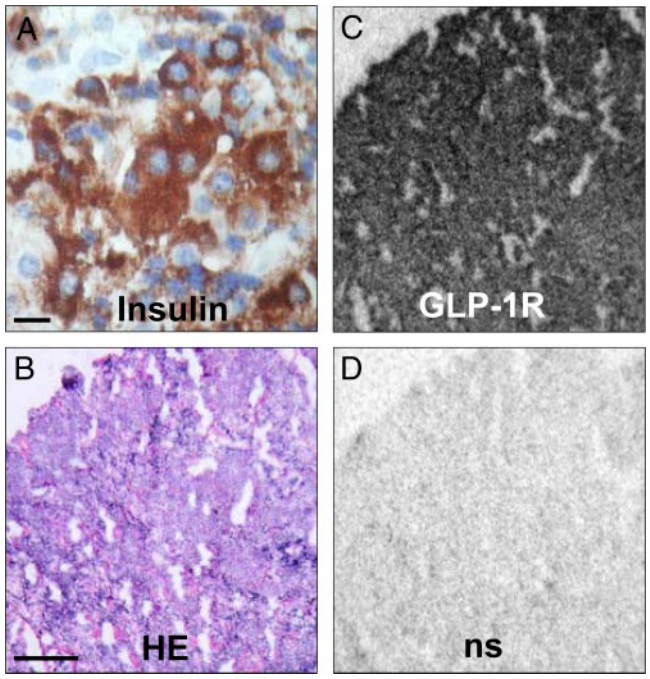

FIG. 4. Hormone and receptor determinations *in vitro* in the insulinoma of patient 5. A, Immunohistochemistry for insulin showing strongly labeled tumor cells. *Bar*, 0.01 mm. B–D, GLP-1R autoradiography. B, Hematoxylin-eosin-stained tumor tissue. *Bar*, 1 mm. C, Autoradiogram showing total binding of ^{125}I-GLP-1 (7–36) amide. Whole tumor is strongly positive. D, Autoradiogram showing nonspecific binding of ^{125}I-GLP-1 (7–36) amide in the presence of 100 nM GLP-1 (7–36) amide.

Histology and autoradiography (Fig. 4)

In all six patients, the diagnosis of benign well-differentiated insulin-producing tumor was confirmed at histology (Fig. 4A). The dimension of the tumors ranged from 9 to 18 mm. Receptor autoradiography of the resected tissues samples showed a very high GLP-1R density in all tested cases (Table 2). This strongly indicated that the hot spots detected by *in vivo* imaging at the tumor site were related to GLP-1R. Figure 4 (B–D) illustrates the GLP-1R expression seen by receptor autoradiography in the tumor of patient 5. Furthermore, two insulinomas expressed *in vitro* low levels of somatostatin receptors: sst_1 receptors (patient 3) and sst_1 and sst_3 receptors (patient 5) were detected, whereas the other subtypes, including sst_2, were absent, indicating that OctreoScan would have been negative in this series of patients (Table 2).

Discussion

This is the first report that provides the proof of concept that ^{111}In-DOTA-exendin-4 is a sensitive tool in preoperatively localizing small intra- and extrapancreatic insulinomas in humans. Furthermore, the precise intraoperative localization of insulinoma using a γ-probe is highly beneficial for the surgical strategy.

Remarkably GLP-1R scintigraphy correctly detected the insulinoma in all six consecutive patients. This novel technique is more sensitive than conventional CT or MRI that detected a suspicious lesion in only one patient, whereas endosonography suggested a lesion in four patients. These conventional imaging data are consistent with previous reports indicating a detection rate of about 60% for MRI or CT scan (23), whereas for endosonography sensitivities up to 80–90% are reported (5, 20). ASVS was performed in three of six patients. This procedure reliably identified the area of localization of the insulinoma in all three patients, in keeping with previous results of the same institution (7). However, the results of ASVS always indicate only the region of the pancreas in which the insulinoma should be located and not the tumor itself. This region is related to the vascular territory of the corresponding artery (7). In patient 2, the results of the ASVS correctly suggested an insulinoma within the region supplied by the anterior mesentery artery, but because this patient had an ectopic insulinoma within the mesentery, the results of the ASVS without GLP-1R imaging would have been misleading for the surgical strategy. Finally, GLP-1R scintigraphy may be superior to the recently reported ^{18}F-DOPA-PET imaging (24) because tumor to pancreas uptake ratios are higher for ^{111}In-DOTA-exendin-4 SPECT than for ^{18}F-DOPA PET (3.3 *vs.* 1.4).

One strength of the current study is the concomitant determination of GLP-1R *in vitro* and *in vivo* using ^{111}In-DOTA-exendin-4. The *in vitro* data clearly indicate that the *in vivo* hot spots correspond to the GLP-1R of the insulinomas. GLP-1R density as assessed in the current study by autoradiography is highly consistent with previous results (12). In general, for *in vivo* tumor targeting, receptor density is critical for sensitivity of the technique (25). This explains the high sensitivity of ^{111}In-DOTA-exendin-4 as reported in the current study.

Within a time frame of 2–14 d after injection of ^{111}In-DOTA-exendin-4, intraoperative use of a γ-probe was highly beneficial for the *in situ* localization in all patients (Fig. 3 and Table 2). It influenced the surgical procedure in four of six patients that permitted a successful enucleation of the insulinoma and detected the ectopic insulinoma. In contrast, the traditional gold standard, *i.e.* intraoperative ultrasound with manual palpation, yields a sensitivity of only about 80% and is not helpful in ectopic insulinoma (1).

Fortunately, GLP-1R scans showed a high tumor to background ratio in all patients. Background uptake over the whole body was low with the exceptions of the kidneys, which were strongly labeled owing to renal excretion of the radioligand. In patients 4 and 6, demarcation between tumors with a maximal diameter of 9–11 mm and kidneys was possible only after late scans, indicating an improved tumor to kidney ratio with time. In fact, the effective half-life of ^{111}In-DOTA-exendin-4 was longer in the tumor (38–64 h) than the kidneys (31.2–31.8 h). This suggests that patients with negative early scans should have additional imaging 3–7 d after the injection. Furthermore, in two patients (patients 2 and 6), there was focal ^{111}In-DOTA-exendin-4 uptake in the proximal duodenum (Fig. 2D). This finding may be related to the fact that the Brunner's gland of the duodenum expresses GLP-1R in high density (21).

In conclusion, these data, although based on a limited number of consecutively enrolled patients, strongly suggest that GLP-1R scintigraphy offers a new approach that permits the successful localization of small insulinomas pre- and intraoperatively. Because virtually all insulinomas express GLP-1Rs, it is likely that this approach will affect the algorithm of pre- and intraoperative localization of suspected insulinoma. It is expected that the success rate of this new technique is very high.

Acknowledgments

We thank Beatrice Waser (Bern) and Priska Preisig, Ksenija Kocur, Andreea Popescu, and Mia Nagy (University Hospital Basel) for excellent technical assistance in carrying out the *in vitro* and scintigraphic work. We also thank Thomas Pfammatter and Christoph Schmid (University Hospital of Zurich) for performing and interpreting the ASVS in three patients, Jan Müller-Brand (University Hospital of Basel) for the SPECT/CT reporting, and Igor Langer and Martin Bosch (Division of Visceral Surgery, University Hospital of Basel, Bruderholzspital) for carrying out surgery in two patients. D.W. and H.M. also acknowledge the support of the European Molecular Imaging Laboratories, a 6th framework program.

Address all correspondence and requests for reprints to: Jean Claude Reubi, M.D., Division of Cell Biology and Experimental Cancer Research, Institute of Pathology, University of Bern, P.O. Box 62, Murtenstrasse 31, CH-3010 Bern, Switzerland. E-mail: reubi@pathology.unibe.ch.

This work was supported by Oncosuisse Grant OCS-01778-08-2005 (to D.W., H.M., and J.C.R.), the Swiss National Science Foundation Grants 320000-109522 (to E.C.) and PASMP3-123269 (to DW).

Disclosure Summary: The authors have no conflict of interest.

References

1. **Grant CS** 2005 Insulinoma. Best Pract Res Clin Gastroenterol 19: 783–798
2. **Service FJ** 1995 Hypoglycemic disorders. N Engl J Med 332:1144–1152
3. **de Herder WW, Niederle B, Scoazec JY, Pauwels S, Kloppel G, Falconi M, Kwekkeboom DJ, Oberg K, Eriksson B, Wiedenmann B,**

Rindi G, O'Toole D, Ferone D 2006 Well-differentiated pancreatic tumor/carcinoma: insulinoma. Neuroendocrinology 84:183–188
4. **Chatziioannou A, Kehagias D, Mourikis D, Antoniou A, Limouris G, Kaponis A, Kavatzas N, Tseleni S, Vlachos L** 2001 Imaging and localization of pancreatic insulinomas. Clin Imaging 25:275–283
5. **Rostambeigi N, Thompson GB** 2009 What should be done in an operating room when an insulinoma cannot be found? Clin Endocrinol (Oxf) 70:512–515
6. **Placzkowski KA, Vella A, Thompson G, Grant CS, Reading CC, Charboneau JW, Andrews JC, Lloyd RV, Service FJ** 2009 Secular trends in the presentation and management of functioning insulinoma at the Mayo Clinic, 1987–2007. J Clin Endocrinol Metab 94:1069–1073
7. **Wiesli P, Brändle M, Schmid C, Krähenbuhl L, Furrer J, Keller U, Spinas GA, Pfammatter T** 2004 Selective arterial calcium stimulation and hepatic venous sampling in the evaluation of hyperinsulinemic hypoglycemia: potential and limitations. J Vasc Interv Radiol 15:1251–1256
8. **Guettier J, Kam A, Chang R, Skarulis MC, Chochran C, Alexander HR, Libutti SK, Pingpank JF, Gorden P** 2009 Localization of insulinomas to regions of the pancreas by intraarterial calcium stimulation: the NIH experience. J Clin Endocrinol Metab 94:1074–1080
9. **Reubi JC** 2003 Peptide receptors as molecular targets for cancer diagnosis and therapy. Endocr Rev 24:389–427
10. **Krenning EP, Kwekkebom DJ, Pauwels S, Kvols LK, Reubi JC** 1995 Somatostatin receptor scintigraphy. In: LM Freeman, ed. Nuclear medicine annual. New York: Raven Press; 1–50
11. **Modlin IM, Oberg K, Chung DC, Jensen RT, de Herder WW, Thakker RV, Caplin M, Delle Fave G, Kaltsas GA, Krenning EP, Moss SF, Nilsson O, Rindi G, Salazar R, Ruszniewski P, Sundin A** 2008 Gastroenteropancreatic neuroendocrine tumours. Lancet Oncol 9:61–72
12. **Reubi JC, Waser B** 2003 Concomitant expression of several peptide receptors in neuroendocrine tumors as molecular basis for *in vivo* multireceptor tumor targeting. Eur J Nucl Med 30:781–793
13. **Mayo KE, Miller LJ, Bataille D, Dalle S, Göke B, Thorens B, Drucker DJ** 2003 International Union of Pharmacology. XXXV. The glucagon receptor family. Pharmacol Rev 55:167–194
14. **Holst JJ** 2007 The physiology of glucagon-like peptide 1. Physiol Rev 87:1409–1439
15. **Gallwitz B** 2006 Exenatide in type 2 diabetes: treatment effects in clinical studies and animal study data. Int J Clin Pract 60:1654–1661
16. **Estall JL, Drucker DJ** 2006 Glucagon and glucagon-like peptide receptors as drug targets. Curr Pharm Des 12:1731–1750
17. **Wild D, Béhé M, Wicki A, Storch D, Waser B, Gotthardt M, Keil B, Christofori G, Reubi JC, Mäcke HR** 2006 [Lys40(Ahx-DTPA-111In)NH2]exendin-4, a very promising ligand for glucagon-like peptide-1 (GLP-1) receptor targeting. J Nucl Med 47:2025–2033
18. **Wild D, Mäcke H, Christ E, Gloor B, Reubi JC** 2008 Glucagon-like peptide 1-receptor scans to localize occult insulinomas. N Engl J Med 359:766–768
19. **Gotthardt M, Lalyko G, van Eerd-Vismale J, Keil B, Schurrat T, Hower M, Laverman P, Behr TM, Boerman OC, Göke B, Béhé M** 2006 A new technique for *in vivo* imaging of specific GLP-1 binding sites: first results in small rodents. Regul Pept 137:162–167
20. **Pitre J, Soubrane O, Palazzo L, Chapuis Y** 1996 Endoscopic ultrasonography for the preoperative localization of insulinomas. Pancreas 13:55–60
21. **Körner M, Stöckli M, Waser B, Reubi JC** 2007 GLP-1 receptor expression in human tumors and human normal tissues: potential for *in vivo* targeting. J Nucl Med 48:736–743
22. **Reubi JC, Waser B, Schaer JC, Laissue JA** 2001 Somatostatin receptor sst1-sst5 expression in normal and neoplastic human tissues using receptor autoradiography with subtype-selective ligands. Eur J Nucl Med 28:836–846
23. **McAuley G, Delaney H, Colville J, Lyburn I, Worsley D, Govender P, Torreggiani WC** 2005 Multimodality preoperative imaging of pancreatic insulinomas. Clin Radiol 60:1039–1050
24. **Kauhanen S, Seppänen M, Minn H, Gullichsen R, Salonen A, Alanen K, Parkkola R, Solin O, Bergman J, Sane T, Salmi J, Välimäki M, Nuutila P** 2007 Fluorine-18-L-dihydroxyphenylalanine (18F-DOPA) positron emission tomography as a tool to localize an insulinoma or β-cell hyperplasia in adult patients. J Clin Endocrinol Metab 92:1237–1244
25. **Kwekkeboom DJ, Bakker WH, Kam BL, Teunissen JJ, Kooij PP, de Herder WW, Feelders RA, Eijck CH, de Jong M, Srinivasan A, Erion JL, Krenning EP** 2003 Treatment of patients with gastro-entero-pancreatic (GEP) tumours with the novel radiolabelled somatostatin analogue [177Lu-DOTA(0), Tyr3]octreotate. Eur J Nucl Med Mol Imaging 30:417–422